Identification of lead compounds targeting the dTDP-L-rhamnose biosynthesis pathway using *Streptococcus pyogenes*

Samantha L. van der Beek[a], Azul Zorzoli[b], Ebru Çanak[a], Robert N. Chapman[c], Benjamin H. Meyer[b], Geert-Jan Boons[c,d], Helge C. Dorfmueller[b,#] and Nina M. van Sorge[a,#]

a. University Medical Center Utrecht, Utrecht University, Medical Microbiology, Heidelberglaan 100, 3584 CX, Utrecht, The Netherlands.

b. Division of Molecular Microbiology, University of Dundee, School of Life Sciences, Dow Street, DD1 5EH, Dundee, UK.

c. Complex Carbohydrate Research Center, Department of Chemistry, The University of Georgia, 315 Riverbend Road, Athens, USA

d. University Utrecht, Utrecht Institute Pharmaceutical Science, Department of Medical Chemistry and Chemical Biology, 3508 TB, Utrecht, The Netherlands

Address correspondence to NM van Sorge, nsorge3@umcutrecht.nl and HC Dorfmueller, h.c.z.dorfmueller@dundee.ac.uk

Running Head: Identifying dTDP-L-rhamnose biosynthesis inhibitors

Abstract

Biosynthesis of the nucleotide sugar precursor dTDP-L-rhamnose is critical for the viability and virulence of many human pathogenic bacteria, including *Streptococcus pyogenes* (Group A *Streptococcus*; GAS) and *Streptococcus mutans*. Both pathogens require dTDP-L-rhamnose for the production of a structurally similar rhamnose-containing polysaccharide in their cell wall. Via heterologous expression in *S. mutans*, we confirm that GAS RmlB and RmlC are critical for dTDP-L-rhamnose biosynthesis through their action as dTDP-glucose-4,6-dehydratase and dTDP-4-keto-6-deoxyglucose-3,5-epimerase enzymes, respectively. Complementation with GAS RmlB and RmlC containing specific point mutations corroborated the conservation of previous identified amino acids in the catalytic site of these enzymes. Bio-layer interferometry was used to identify inhibitory lead compounds that bind directly to GAS dTDP-rhamnose biosynthesis enzymes RmlB, RmlC and GacA in a concentration-dependent manner. One of the identified compounds, Ri03, inhibited growth of GAS as well as several other streptococcal pathogens with an MIC_{50} of 120-410 µM. Ri03 displayed no cytotoxity in U937 monocytic cells up to a concentration of 15 mM. We therefore conclude that Ri03 can serve as a lead compound for the development of a new class of antibiotics that targets dTDP-rhamnose biosynthesis in pathogenic bacteria.

Introduction

The typical cell wall architecture of a Gram-positive bacterium consists of a thick peptidoglycan layer decorated with wall teichoic acids, proteins and capsular polysaccharides. However, certain lactic acid bacteria, particularly streptococcal species, lack the expression of wall teichoic acids and instead express a rhamnose cell wall polysaccharide, which is covalently anchored to peptidoglycan (1). Rhamnose cell wall polysaccharides encompass about 40-60% of the cell wall mass and are considered as functional homologs of wall teichoic acids (2, 3). Examples of rhamnose cell wall polysaccharides are the group A carbohydrate (GAC) of *Streptococcus pyogenes* (Group A *Streptococcus*; GAS) and the serotype-determining polysaccharides, referred to as rhamnose-glucose polysaccharide (RGP), of *Streptococcus mutans*. The GAC and RGP share structural similarities; both consist of an α-1,2-/α-1,3-linked polyrhamnose backbone with alternating *N*-acetylglucosamine for GAS and glucose or galactose side chains for *S. mutans* (4-8) (Fig. 1). For *S. mutans*, the type of side chain as well as their linkage to the rhamnan backbone determines the *S. mutans* serotype (6, 9) (Fig. 1). In contrast, all GAS serotypes express a structurally invariant GAC (10). Similar to classical wall teichoic acids, rhamnose cell wall polysaccharides are critical for maintaining cell wall shape, bacterial physiology and virulence, but in-depth knowledge of their biosynthesis or host interactions at a molecular level is limited (11-14). A better understanding of these mechanisms could aid the development of new classes of antibiotics, antibiotic adjuvants or vaccines (6, 12, 15).

L-Rhamnose is the main building block for both the GAC and RGP. The biosynthesis pathway of the nucleotide precursor, dTDP-L-rhamnose, is highly conserved among both Gram-positive and Gram-negative bacteria (1, 16). The dTDP-L-rhamnose biosynthesis pathway is critical or even essential for viability or virulence of a wide range of human pathogens including GAS (17, 18), Group B *Streptococcus* (GBS) (2, 19), some serotypes of *Streptococcus pneumoniae* (20, 21), *S. mutans* (13, 22-24), *Enterococcus faecalis* (25, 26), *Mycobacterium spp.* (27, 28), *Pseudomonas spp.* (29) and *Salmonella enterica* serovar *Typhimurium* (30). Consequently, this pathway is considered to be an

interesting drug target, especially since dTDP-L-rhamnose is not produced or used by humans (31). dTDP-L-rhamnose is produced through a four-step enzymatic pathway catalyzed by the enzymes RmlA-D. The mechanisms of action as well as structural characteristics of the RmlA-D enzymes have been studied extensively (11, 32-40). Indeed, crystal structures are available for all four Rml enzymes from different Gram-positive and Gram-negative bacterial species and show high structural conservation. This structural and functional information has enabled the development of different screening methods to discover inhibitors against RmlB-D, yielding compounds that can inhibit dTDP-L-rhamnose biosynthesis in the low micromolar range in a biochemical assay (41-45).

Recently, we characterized GAS GacA as an RmlD homolog catalyzing the last step in dTDP-L-rhamnose biosynthesis (11). Surprisingly, this GAS RmlD enzyme was confirmed to be a monomer as opposed to previously characterized RmlD dimers. Additional bioinformatics analysis of 213 RmlD homologs revealed that the majority of RmlD enzymes are predicted to be monomeric, while only a subclass of RmlD enzymes in Gram-negatives form metal-dependent homodimers (46). In this study, we extended our work to study GAS RmlB and RmlC on a functional level through heterologous expression in *S. mutans* and subsequent analysis of growth, morphology and cell wall composition. In addition, we report the identification of small chemical compounds that target these enzymes. These compounds inhibited growth of GAS in a sub- to low-millimolar range, however several compounds showed off-target effects. Compound Ri03 is considered to be the most promising new lead compound due to its minimal off-target effects and low toxicity towards eukaryotic cells. These results demonstrate that rhamnose biosynthesis inhibitors can directly interfere with bacterial viability and could form a new class of antibiotics targeting nucleotide sugar production.

Results

Protein sequence analysis of GAS RmlB and RmlC

As an extension of our previous work on GAS GacA (11), we sought to characterize GAS RmlB (GAS5448_RS05645) and RmlC (GAS5448_RS05650), the putative dTDP-glucose-4,6-dehydratase and dTDP-4-keto-6-deoxyglucose-3,5-epimerase, respectively. GAS *rmlB* and *rmlC* are clustered in an operon together with *rmlA* in the order *rmlA-rmlC-rmlB*. Structural and biochemical analysis of RmlB and RmlC from *S. suis*, *S. enterica* and *M. tuberculosis* revealed that both enzymes are functional homodimers in these organisms (33-37). Protein sequence alignment of streptococcal and *S. enterica* RmlB and RmlC homologs displayed a high homology (Fig. 2). Importantly, all catalytic residues in RmlB and RmlC are conserved (Fig. 2).

GAS RmlB and RmlC functionally replace *S. mutans* homologs

Most genes directly or indirectly involved in the GAC biosynthesis pathway are essential for GAS viability, including all four dTDP-L-rhamnose biosynthesis genes *rmlA-C* and *gacA* (11, 14, 17, 18). In contrast, the dTDP-L-rhamnose biosynthesis genes are not essential in *S. mutans*, although gene deletions result in attenuated growth and severe morphological defects (11, 47). GAS RmlB and RmlC proteins share 94% and 83% protein sequence identity with the *S. mutans* homologs, respectively. In addition, the organization of these genes is identical in both species, consisting of one operon together with RmlA. Interestingly, *S. mutans* strains contain a hypothetical protein (174 nucleotides, 57 amino acids) encoded between RmlC and RmlB.

To confirm the function of GAS RmlB and RmlC in dTDP-L-rhamnose biosynthesis, we heterologously expressed GAS RmlB and GAS RmlC-encoding genes in *S. mutans* strains lacking *rmlB* or *rmlC*, respectively. Deletion of *S. mutans rmlB* (SMU Δ*rmlB*) or *rmlC* (SMU Δ*rmlC*) by replacement with an erythromycin resistance cassette severely attenuated bacterial growth compared to the wild-type strain (WT) (Fig. 3A, B), which is characteristic for a rhamnose-deficient *S. mutans* strain and in line

with our previously constructed *S. mutans rmlD* deletion strain (11). In addition, analysis of *rmlB* and *rmlC* mutant bacteria by scanning electron microscopy revealed swelling and clumping of bacteria as a result of misplaced septa resulting in division errors and multidirectional growth (Fig. 3C). Subsequent analysis of the cell wall carbohydrate composition by HPLC/MS confirmed that SMU Δ*rmlB* and SMU Δ*rmlC* lacked rhamnose in their cell walls, which concordantly resulted in the loss of the glucose side chains (Fig. 3D). Introduction of either homologous *S. mutans rmlB* or heterologous GAS *rmlB* on an expression plasmid in the corresponding Δ*rmlB* mutant restored rhamnose incorporation in the cell wall as well as the defective morphological phenotype and growth (Fig. 3B-D). Initially, we were unable to complement SMU Δ*rmlC* with *rmlC* from SMU, whereas heterologous GAS *rmlC* could restore SMU Δ*rmlC* growth, morphology and rhamnose production (Fig. 3A, C, D). Upon reexamination of the UA159 genome, a *S. mutans* serotype c strain that we used as a reference genome for *S. mutans* Xc, we located an alternative ATG-start site 135 bp upstream of the annotated *rmlC* gene, which is in line with the annotation of *rmlC* in GAS. Importantly, available structural information indicate that the first 45 amino acids are part of the RmlC dimerization interface, in particular forming the extension of the beta-sheet with two additional beta-strands, which are required for nucleotide binding (34, 48). In agreement with this observation, complementation of SMU Δ*rmlC* with the extended PCR product complemented all observed defects (Fig 3A, C, D), indicating that the longer gene indeed encodes a functional RmlC enzyme (198 amino acids), which is similar to the size of GAS and *S. suis* RmlC (197 amino acids).

Catalytic residues of GAS RmlB and RmlC are conserved

Based on the protein sequence alignment of GAS RmlB and RmlC with the previously published crystal structures of *S. suis* RmlB and RmlC (33, 37), we set out to functionally validate predicted catalytic residues of GAS RmlB (Y159) and RmlC (H76 and K82) through heterologous expression in *S. mutans*. Point mutations were individually introduced in GAS RmlB (Y159F) and RmlC (H76N and K82A) and overexpression vectors carrying these mutant genes were expressed in SMU Δ*rmlB* and SMU Δ*rmlC*, respectively. All mutated residues are involved in catalysis and mutated proteins were

unable to complement the characteristic rhamnose-depleted phenotype consisting of growth retardation and an aberrant morphology (Fig. 3A-C). Complementary, our cell wall composition analysis revealed that the *S. mutans* strains carrying these three point mutants completely lacked incorporation of rhamnose in their cell wall (Fig. 3D).

Inhibitor screen against GAS Rml proteins and hit confirmation

Given the importance of the dTDP-L-rhamnose biosynthesis pathway for viability and/or virulence of many human pathogens, we aimed to identify chemical scaffolds that could act as starting points for future optimization and drug development pipelines. Therefore, we conducted a bio-layer interferometry (BLI) inhibitor screen against the commercially available Maybridge Library using the three recombinant GAS dTDP-rhamnose biosynthesis enzymes RmlB, RmlC and GacA (Fig. S1A). The advantage of this approach is that it precludes the use of expensive or commercially unavailable enzyme substrates. Using a commercially available library of ~1,000 compounds, our initial screen identified 12 hits of which seven compounds were found to specifically interact with GAS RmlB/RmlC/GacA as confirmed by BLI (Fig. S1B-D). In addition, we confirmed the identified hits in dilution series for their binding affinity to these three enzymes (Fig. S2, Table S3). Importantly, this method allowed us to estimate enzyme specificity by comparing the data obtained from one enzyme to the other two. This way, we identified chemical scaffolds with specificity for one enzyme, but also several compounds that bound to more than one enzyme of the dTDP-rhamnose biosynthesis pathway (Tables 1 and S3, Fig. S2).

Bactericidal activity of identified compounds

Since dTDP-rhamnose is an essential nucleotide sugar in GAS, we assessed the functional capacity of these compounds to impact GAS growth. All compounds identified in this study were water insoluble and were therefore dissolved in DMSO, except Ri07, which was already liquid at room temperature. GAS is tolerant to DMSO concentrations of 2%, therefore this was the maximum concentration used in bacterial assays. Even in DMSO, Ri04 and Ri07 were highly insoluble in bacterial culture medium

and could therefore not be tested for inhibition of bacterial growth. The remaining five compounds were able to inhibit growth of GAS with MIC_{50} values ranging from 110 µM to 6.2 mM (Fig. 4A, Table 1). In accordance with growth inhibition, GAS morphology was also severely affected upon exposure to either 200 µM Ri03 or 100 µM Ri06 (Fig. 4B). Especially for Ri03, streptococci were swollen and chains were longer, a phenotype corresponding to an inducible *gacA* GAS knock-out strain (11).

Target specificity of potential inhibitors

We aimed to gain more insight into target specificity of these five compounds. Therefore, we assessed whether Ri01, Ri02, Ri03, Ri06 and Ri08 inhibited growth of *S. aureus* USA300 NRS384, a pathogenic methicillin-resistant bacterium that lacks expression of rhamnose (Fig. 5A, Table 1). Four of the five compounds only showed 2- or 4-fold differences in MIC_{50} compared to GAS. However, compound Ri03 inhibited growth of GAS ~20-fold more effective compared to *S. aureus* (120 µM vs. 2.48 mM). We also assessed growth inhibition on an *E. coli* strain that produces non-essential rhamnose (49) as confirmed by deletion of *rfbA*, an *rmlA* homolog, which did not affect the growth rate. Similar to *S. aureus*, Ri03 was approximately 30-fold less effective on this *E. coli* compared to GAS with an MIC_{50} of 3.61 mM (Table 2, Fig. S3A) and was not affected by mutation of *rfbA* (Table 2, Fig. S3A), suggesting that the observed growth inhibition, both in *E. coli* and *S. aureus*, is due to off-target effects of Ri03.

Ri03 prevents growth of other pathogenic streptococci

The observed window in Ri03 efficacy between GAS and *E. coli*/*S. aureus* suggested that Ri03-mediated growth inhibition is partially dependent on inhibition of dTDP-L-rhamnose biosynthesis. We therefore extended our experiments to include other human and animal streptococcal species for which dTDP-rhamnose is an essential nucleotide sugar. Group C *Streptococcus* (GCS; *Streptococcus equi*) contains a related surface carbohydrate, the characteristic Group C Carbohydrate, composed of a polyrhamnose backbone decorated with a GalNAc (1). Ri03 inhibited

growth of GCS with an MIC_{50} of 0.42 mM (Table 2, Fig. S3B). Furthermore, Ri03 was able to prevent growth of *S. mutans* with an MIC_{50} of 0.41 mM (Table 2, Fig. S3B).

Cytotoxicity of Ri03 in human U937 cells

Human cells do neither produce L-rhamnose nucleotide sugars, nor is there any evidence for them incorporating L-rhamnose into their carbohydrates (31). Nonetheless, blasting of bacterial rhamnose biosynthesis enzyme sequences against the human genome revealed a possible human homolog of RmlB. The human gene *TGDS* is annotated to encode a dTDP-glucose-4,6-dehydratase, which shares 33-36% protein sequence identity with Gram-positive and Gram-negative RmlB enzymes (Fig. S4A, B). We therefore investigated whether TGDS could act as a functional RmlB homolog by complementing SMU Δ*rmlB* with codon-optimized *TGDS*, which should assist the production of TGDS in bacterial cells, on an expression plasmid. However, TGDS was not able to complement the attenuated growth rate or aberrant morphology of SMU Δ*rmlB* (Fig. S4C).

Given potential presence of structural homologs in eukaryotic cells, Ri03 was tested for cytotoxicity on U937 cells, a human monocytic cell line, by measuring the release of lactose dehydrogenase (LDH) into the supernatant. Ri03 induced 5% LDH release with a concentration of 20 mM Ri03 (Fig. 5B). LDH release was comparable to DMSO controls for concentrations up to 15 mM. Compared to the MIC_{50} of Ri03 on GAS (120 µM), there is a therapeutic window of more than 150-fold.

Discussion

In this study we show that GAS RmlB and RmlC are the dTDP-glucose-4,6-dehydratase and dTDP-4-keto-6-deoxyglucose-3,5-epimerase enzymes, respectively. Both GAS RmlB and RmlC functionally replaced *S. mutans* homologs in a heterologous expression system. Also, deletion of each individual gene in *S. mutans* resulted in a phenotype similar as previously observed for an *rmlD* deletion mutant (11), suggesting that inhibition of the dTDP-rhamnose biosynthesis pathway severely impacts bacterial viability. Our study therefore shows that *S. mutans* does not have a salvage

pathway to rescue *rml* deletions. In addition to proving the function of both GAS RmlB and RmlC as rhamnose biosynthesis enzymes, we also identified Y159 in RmlB and H76 and K82 in RmlC as critical catalytic residues. Our complementation studies indicate that the mechanism of catalysis is conserved among streptococcal species.

Screening a chemical compound library to identify inhibitors of the dTDP-L-rhamnose biosynthesis pathway is methodically challenging. Previously, indirect methods were used to determine the production of the end product dTDP-L-rhamnose by monitoring the production of co-factor NAD(P)H (11, 44, 50). Alternatively, a superior assay would involve a HPLC or mass-spectrometry approach where every single step of product formation and substrate consumption could be monitored. However, it is very challenging to develop this method suitable for medium or high throughput screening. We therefore investigated an approach using recombinant enzymes in their natural state, i.e. with bound co-factors in their active site. RmlB enzymes require the co-factors NAD(P), which appears to be tightly bound in the active site as it was co-purified during RmlB crystallizations (35, 38). This is in agreement with the regeneration of NAD during dTDP-4-keto-6-deoxy-D-glucose synthesis (38). GacA/RmlD enzymes also require NADPH as a co-factor, which appears to be less tightly bound as it was not observed in the GAS GacA and *S. suis* RmlD crystal structures and therefore should be regenerated by a different enzyme (11, 46). Using the binding approach, we identified seven inhibitors that interacted with at least one enzyme of the dTDP-L-rhamnose biosynthesis pathway with low millimolar to high micromolar affinities. One of the most potent chemical fragments Ri03, 5-(4-chlorophenyl)-2-furoic acid, is a small molecule, which binds RmlB and GacA in the high µM range, and RmlC in the low millimolar range. We show that Ri03 is able to prevent growth of several streptococcal strains, which express rhamnose as an essential component of their cell wall. The high sequence identity of RmlB and GacA/RmlD amongst GAS, GCS and *S. mutans* (92-94% and 82-87% protein sequence identity, respectively; Fig. 2C) supports the observation that Ri03 shows similar MIC_{50} values against all three strains. Importantly, Ri03 only inhibits growth in the millimolar range of species that do not produce rhamnose (*S. aureus*) or for

which rhamnose is not essential (*E. coli*). This data suggests that compound Ri03 has, in addition to on-target effects, also minor off-target effects for which the targets remain unknown.

To our surprise, bioinformatics revealed that the human protein TGDS shares 33-36% protein sequence identity with bacterial RmlB enzymes and has previously been annotated as a dTDP-glucose-4,6 dehydratase (51). It seems unlikely that this annotation for TGDS is correct, considering that both dTDP-L-rhamnose and dTDP-D-glucose, the substrate of RmlB, have not been detected in human cells (31, 52). In support of this, we were unable to complement SMU Δ*rmlB* with codon-optimized *TGDS*. However, it remains unknown whether TGDS was produced as a functional enzyme and whether it is a promiscuous enzyme that is able to convert dTDP-glucose into dTDP-4-keto-6-deoxy-D-glucose. We therefore advise to test potential inhibitors against RmlB, such as Ri03, for binding to TGDS to exclude off target effects as a precautionary measure, given that mutations in TGDS cause the rare Catel-Manzke syndrome (Fig. S4A) (51, 53, 54).

Our initial studies to test off-target toxicity of Ri03 in U937 human monocytic cells showed no cytotoxicity with concentrations up to 15 mM. Certainly, more studies are required with Ri03 and subsequent derivatives to further assess potential cytotoxicity towards human cells. However, these first results suggest a reasonable therapeutic window, which may be increased after additional optimization of this chemical scaffold. Future experiments aim to investigate the binding mode of Ri03 on a structural level to the proteins RmlB, RmlC and GacA. These complex and challenging tasks will reveal new insights, in particular whether Ri03 inhibits RmlB, RmlC and GacA by competing with the nucleotide-sugar and if a common binding mode is observed amongst the different enzymes. Furthermore, these studies will greatly enhance our understanding to elucidate commercial derivatives of Ri03 that will be explored to identify more potent derivatives targeting the GAS and related homologues enzymes. At the same time, these future studies will allow conducting structure-based drug design approaches, and designing and synthesizing novel derivatives with greater potency targeting GAS and related pathogens.

Materials and Methods

Bacterial strains and growth conditions

Bacterial strains used in this study are described in Table 3. *Streptococcus mutans* Xc (55), a serotype c wild-type (WT) strain, was a kind gift of Dr. Y. Yamashita (Kyushu University, Japan) and was routinely grown in Todd-Hewitt Broth (THB, Oxoid) or on THB agar at 37°C with 5% CO_2. When appropriate, *S. mutans* was cultured with 10 µg/ml erythromycin (ERY) or 3 µg/ml chloramphenicol (CHL). Group A *Streptococcus* 5448 (GAS), a representative of the epidemic M1T1 clone, was cultured in Todd-Hewitt Broth (Becton Dickinson) supplemented with 1% yeast extract (THY; Oxoid) or on THY agar at 37°C. *E. coli* MC1061 was used for cloning purposes and was grown in lysogeny broth (LB, Oxoid) or on LB agar containing 10 µg/ml CHL at 37 °C.

Cloning, expression and purification of GAS enzymes

GAS RmlB, RmlC and GacA proteins were produced and purified as described previously (11).

Genetic manipulation of SMU

S. mutans is naturally competent and was transformed as described previously. Shortly, bacteria were grown in THB containing 5% heat-inactivated horse serum (BioRad) and supplied with 500 ng knockout construct or complementation plasmid (11). Cultures were plated on THB agar plates containing the appropriate antibiotics. Single colonies were selected and verified for the deletion of *rmlB*/*rmlC* and/or the presence of complementation plasmid using colony PCR and sequencing.

Deletion mutants of *rmlB* (SMU Δ*rmlB*) and *rmlC* (SMU Δ*rmlC*) were obtained via the addition of a knockout construct to *S. mutans* WT. This construct consisted of an ERY resistance cassette with ~700 bp flanking regions homologous to the up- and downstream regions of *rmlB* or *rmlC*. A detailed cloning strategy is available in the supplemental material and Table S1.

S. mutans complementation plasmids

S. mutans rmlB/rmlC and GAS *rmlB/rmlC* were amplified from gDNA using primers containing XbaI, XhoI or BamHI restriction site (Table S1). Digested PCR products were subsequently ligated into expression plasmid pDC123 and propagated in *E. coli* MC1061 to obtain large quantities of complementation plasmid. Point mutations were introduced by mutagenesis PCR, using overlapping primers with the corresponding mutation site integrated. The constructed plasmids with the single point mutations were all confirmed by DNA sequencing.

For complementation of SMU Δ*rmlB* with the human gene *TGDS* (gene ID: 23483), the exons of *TGDS* were first codon optimized for SMU UA159. A gBlock of this optimized sequence with XbaI-pDC123 and BglII-pDC123 overhangs attached to the 5'- and 3'-ends, respectively, was used to ligate TGDS into pDC123 (pTGDS), which was confirmed by DNA sequencing.

SMU Δ*rmlB* and SMU Δ*rmlC* knockout mutants were not transformable likely due to the severe growth defects. Therefore, SMU Δ*rmlB* and SMU Δ*rmlC* strains complemented with *S. mutans rmlB/rmlC* or GAS *rmlB/rmlC* were constructed using a two-step approach. First, *S. mutans* WT was transformed with the complementation plasmid as described above. Next, these complemented strains were transformed with the respective *rmlB* or *rmlC* knockout constructs and selected for double antibiotic resistance.

Scanning Electron Microscopy

Scanning electron microscopy was performed as described previously by van der Beek et al (11). In short, bacteria were grown to mid-exponential phase, except when incubated with rhamnose inhibitor. In this case, bacteria were cultured as described below in bacterial growth inhibition assays and grown overnight. Bacteria were subsequently washed, fixed, dehydrated, mounted onto 12.5 mm specimen stubs (Agar scientific, Stansted, Essex, UK) and coated with gold to 1 nm using a Quorum Q150R S sputter coater at 20 mA. Samples were visualized with a Phenom PRO desktop scanning electron microscope (Phenom-World BV) at an acceleration voltage of 10 kV.

S. mutans growth curves

Overnight cultures of *S. mutans* strains with an optical density at 600 nm (OD_{600}) higher than 0.35 were diluted 10 times and grown for 1.5 h to early exponential phase. Cultures were then diluted to OD_{600} 0.03 and OD_{600} was measured manually every 30 min. For cultures with an overnight OD_{600} below 0.35, the initial 10-fold dilution and growth step was omitted. Instead, such overnight cultures were directly diluted to OD_{600} 0.03 and OD_{600} was measured every hour. All cultures were incubated at 37 °C with 5% CO_2 in between measurements.

Cell wall carbohydrate composition analysis

Cell wall polysaccharides were isolated from *S. mutans,* hydrolyzed and analyzed by chromatography as described previously by van der Beek *et al*. (11). In short, bacterial cells were harvested from 2-5 L cultures and disrupted in 0.1 M citrate buffer (pH 4.6) using a bead beater (Biospec). Cell walls were collected by centrifugation and boiled for 1 h at 100 °C in 0.1 M sodium acetate (pH 4.6) containing 4% sodium dodecyl sulfate. Samples were subsequently treated with RNase, DNase, pronase E and trypsin. Cell wall polysaccharides containing peptidoglycan and the serotype c carbohydrate were lyophilized before hydrolysis with TFA. Finally, carbohydrate analysis of monosaccharides was performed on a Dionex ICS-3000 Ion Chromatography System (Dionex / Thermo Scientific, 1228 Titan Way, P.O. Box 3603, Sunnyvale, CA, 94088-3603, United States) using a CarboPac PA20 (Dionex / Thermo Scientific, 1228 Titan Way, P.O. Box 3603, Sunnyvale, CA, 94088-3603, United States) 3 × 150 mm column, equipped with a ICS-3000 Electrochemical Detector (Dionex / Thermo Scientific, 1228 Titan Way, P.O. Box 3603, Sunnyvale, CA, 94088-3603, United States). Monosaccharides from all samples were eluted from the column with 12% 0.2 M NaOH, except for monosaccharides from SMU Δ*rmlB* and Δ*rmlC*, which were eluted with 8% 0.2 M NaOH. The 'Carbohydrates (Standard Quad)' waveform was used for detection.

BLI screen using recombinant RmlB, RmlC and GacA

The Maybridge library of fragment-like molecules (Ro3) was purchased from Maybridge (USA). All three GAS proteins, RmlB, RmlC and GacA, were screened against the library using identical protocols. Proteins were biotinylated on primary amine amino acid side chains using the Thermo Scientific™ EZ-Link™ NHS-PEG$_4$-Biotin reagent. The enzymes were incubated with NHS-PEG$_4$-Biotin in a 1:1 molar ratio at 150 µM for 45 min at room temperature. The reaction buffer contained 25 mM HEPES, pH 7.5, 150 mM NaCl and 0.02 mM TCEP. Excess NHS-PEG$_4$-biotin reagent was removed using 2 mL Zeba desalting spin columns (Thermo Scientific). Successful biotinylation on primary amines was investigated via Western blotting and probing with ExtrAvidin®–Peroxidase antibody, 1:10,000 (Sigma E2886, Fig. S1A). Before compound screening, the proteins were loaded onto a parallel set of superstreptavidin biosensors (SSA) by incubation in buffer for 900 sec. Protein concentrations suitable for the experiments were determined in a series of dilutions. Final screening was conducted at concentrations of: 50 µg/mL RmlB, 25 µg/mL RmlC and 12.5 µg/mL GacA. All compounds were at 2% DMSO concentration. The sensor was blocked by immersion in biocytin (10 µg/mL) for 30 sec.

Initial library screening was performed at a compound concentration of 200 µM. Hits were identified by plotting the response rate of every single compound after background subtraction. In total, 12 compounds were validated in 6-point concentration series using 3-fold dilutions, ranging from 670 µM to 3 µM. Data were processed and kinetic parameters were calculate using the ForteBio software. Binding curves were manually inspected and approximate binding constants K_D are listed in Table S3.

Bactericidal activity

GAS 5448, *S. aureus* NRS384, several *E. coli* strains, GCS MGCS10565 and *S. mutans* Xc strains (Table 3) were grown in appropriate bacterial culture broth overnight at 37 °C. Bacterial cultures were diluted 10 times and grown to mid-log phase (OD_{600} 0.4). Cultures were diluted 200 times in culture

medium followed by a 2-fold dilution with various concentrations of rhamnose inhibitor or DMSO. OD_{600} was recorded every 15 min at 37°C with 5 sec medium shaking before measurement for GAS, GCS, *S. mutans* and *E. coli* or medium continuous shaking for *S. aureus* using either a Bioscreen C MBR machine (Growth Curves AB Ltd, Oy, Finnland) or a Synergy 2 plate reader (Biotek). OD_{600} values were plotted against the concentration of compound after 9 hours of growth using GraphPad Prism 7. MIC_{50} values were calculated using a non-linear four-parameter dose-response curve with variable slope. Because high concentrations were not always feasible due to solubility issues, a high concentration of compound (50 mM) was artificially introduced where appropriate and set to zero to obtain more reliable dose-response curves.

Cytotoxicity

U937 human monocytic cells (American Type Culture Collection) were grown at 37 °C with 5% CO_2 in RPMI 1640 (Biowest) containing 100 U/ml penicillin (Gibco), 100 µg/ml streptomycin (Gibco) and 5% fetal calf serum (Biowest). Cells were then centrifuged and adjusted to 10^7 cells/ml in THB medium. In a 96-well round bottom plate, 10^5 U937 cells were added to 100 µl of THB containing various concentrations of Ri03, DMSO or lysis buffer. Cells were incubated for 30 min at 37 °C with 5% CO_2 with mild shaking. U937 cells were centrifuged and 50 µl of supernatant was transferred to a new 96-well flat bottom plate. Lactose dehydrogenase release was measured using the CytoTox 96® Non-Radioactive Cytotoxicity Assay kit (Promega) by adding 50 µl of substrate reagent. OD_{490} was measured after 30 min using an iMark™ microplate absorbance reader (Bio-Rad). No stop buffer was added to avoid precipitation of Ri03. Percentage of cytotoxicity is calculated relative to lysis buffer control.

Acknowledgments

The authors would like to acknowledge Dr Olawale Raimi (University of Dundee) for assistance with BLI. We are grateful for funding to HCD and his laboratory from Tenovus Scotland, Wellcome Trust

and Royal Society (grant number 109357/Z/15/Z.), FEBS and the University of Dundee. This work was supported by a VIDI grant (91713303) from the Dutch Scientific Organization (NWO) to N.M.v.S and S.v.d.B. The authors declare no conflict of interest.

References

1. Mistou MY, Sutcliffe IC, van Sorge NM. 2016. Bacterial glycobiology: rhamnose-containing cell wall polysaccharides in Gram-positive bacteria. FEMS Microbiol Rev 40:464-79.

2. Caliot E, Dramsi S, Chapot-Chartier MP, Courtin P, Kulakauskas S, Pechoux C, Trieu-Cuot P, Mistou MY. 2012. Role of the Group B antigen of *Streptococcus agalactiae*: a peptidoglycan-anchored polysaccharide involved in cell wall biogenesis. PLoS Pathog 8:e1002756.

3. Sutcliffe IC, Black GW, Harrington DJ. 2008. Bioinformatic insights into the biosynthesis of the Group B carbohydrate in *Streptococcus agalactiae*. Microbiology 154:1354-1363.

4. Heymann H, Manniello JM, Zeleznick LD, Barkulis SS. 1964. Structure of Streptococcal Cell Walls. Ii. Group a Biose and Group a Triose from C-Polysaccharide. J Biol Chem 239:1656-63.

5. Huang DH, Rama Krishna N, Pritchard DG. 1986. Characterization of the group A streptococcal polysaccharide by two-dimensional 1H-nuclear-magnetic-resonance spectroscopy. Carbohydr Res 155:193-9.

6. St Michael F, Yang Q, Cairns C, Vinogradov E, Fleming P, Hayes AC, Aubry A, Cox AD. 2017. Investigating the candidacy of the serotype specific rhamnan polysaccharide based glycoconjugates to prevent disease caused by the dental pathogen *Streptococcus mutans*. Glycoconj J doi:10.1007/s10719-017-9798-z.

7. Pritchard DG, Gregory RL, Michalek SM, McGhee JR. 1986. Characterization of the serotype e polysaccharide antigen of *Streptococcus mutans*. Mol Immunol 23:141-5.

8. Linzer R, Reddy MS, Levine MJ. 1987. Structural studies of the serotype-f polysaccharide antigen from *Streptococcus mutans* OMZ175. Infect Immun 55:3006-10.

9. Nakano K, Ooshima T. 2009. Serotype classification of *Streptococcus mutans* and its detection outside the oral cavity. Future Microbiol 4:891-902.

10. Lancefield RC. 1933. A Serological Differentiation of Human and Other Groups of Hemolytic Streptococci. J Exp Med 57:571-95.

11. van der Beek SL, Le Breton Y, Ferenbach AT, Chapman RN, van Aalten DM, Navratilova I, Boons GJ, McIver K, van Sorge NM, Dorfmueller HC. 2015. GacA is Essential for Group A *Streptococcus* and Defines a New Class of Monomeric dTDP-4-dehydrorhamnose Reductases (RmlD). Mol Microbiol doi:10.1111/mmi.13169.

12. van Sorge NM, Cole JN, Kuipers K, Henningham A, Aziz RK, Kasirer-Friede A, Lin L, Berends ET, Davies MR, Dougan G, Zhang F, Dahesh S, Shaw L, Gin J, Cunningham M, Merriman JA, Hutter J, Lepenies B, Rooijakkers SH, Malley R, Walker MJ, Shattil SJ, Schlievert PM, Choudhury B, Nizet V. 2014. The classical lancefield antigen of group A *Streptococcus* is a virulence determinant with implications for vaccine design. Cell Host Microbe 15:729-40.

13. Kovacs CJ, Faustoferri RC, Quivey RG, Jr. 2017. RgpF Is Required for Maintenance of Stress Tolerance and Virulence in *Streptococcus mutans*. J Bacteriol 199.

14. Zhu L, Charbonneau ARL, Waller AS, Olsen RJ, Beres SB, Musser JM. 2017. Novel Genes Required for the Fitness of *Streptococcus pyogenes* in Human Saliva. mSphere 2.

15. Sabharwal H, Michon F, Nelson D, Dong W, Fuchs K, Manjarrez RC, Sarkar A, Uitz C, Viteri-Jackson A, Suarez RS, Blake M, Zabriskie JB. 2006. Group A *Streptococcus* (GAS) carbohydrate as an immunogen for protection against GAS infection. J Infect Dis 193:129-35.

16. Giraud MF, Naismith JH. 2000. The rhamnose pathway. Curr Opin Struct Biol 10:687-96.

17. Le Breton Y, Belew AT, Valdes KM, Islam E, Curry P, Tettelin H, Shirtliff ME, El-Sayed NM, McIver KS. 2015. Essential Genes in the Core Genome of the Human Pathogen *Streptococcus pyogenes*. Sci Rep 5:9838.

18. Le Breton Y, Mistry P, Valdes KM, Quigley J, Kumar N, Tettelin H, McIver KS. 2013. Genome-wide identification of genes required for fitness of group A *Streptococcus* in human blood. Infect Immun 81:862-75.

19. Hooven TA, Catomeris AJ, Akabas LH, Randis TM, Maskell DJ, Peters SE, Ott S, Santana-Cruz I, Tallon LJ, Tettelin H, Ratner AJ. 2016. The essential genome of *Streptococcus agalactiae*. BMC Genomics 17:406.

20. Kim JO, Romero-Steiner S, Sorensen UB, Blom J, Carvalho M, Barnard S, Carlone G, Weiser JN. 1999. Relationship between cell surface carbohydrates and intrastrain variation on opsonophagocytosis of *Streptococcus pneumoniae*. Infect Immun 67:2327-33.

21. Magee AD, Yother J. 2001. Requirement for capsule in colonization by *Streptococcus pneumoniae*. Infect Immun 69:3755-61.

22. Engels-Deutsch M, Pini A, Yamashita Y, Shibata Y, Haikel Y, Scholler-Guinard M, Klein JP. 2003. Insertional inactivation of *pac* and *rmlB* genes reduces the release of tumor necrosis factor alpha, interleukin-6, and interleukin-8 induced by *Streptococcus mutans* in monocytic, dental pulp, and periodontal ligament cells. Infect Immun 71:5169-77.

23. Shields RC, Zeng L, Culp DJ, Burne RA. 2018. Genomewide Identification of Essential Genes and Fitness Determinants of *Streptococcus mutans* UA159. mSphere 3.

24. Tsuda H, Yamashita Y, Toyoshima K, Yamaguchi N, Oho T, Nakano Y, Nagata K, Koga T. 2000. Role of serotype-specific polysaccharide in the resistance of *Streptococcus mutans* to phagocytosis by human polymorphonuclear leukocytes. Infect Immun 68:644-50.

25. Xu Y, Singh KV, Qin X, Murray BE, Weinstock GM. 2000. Analysis of a gene cluster of *Enterococcus faecalis* involved in polysaccharide biosynthesis. Infect Immun 68:815-23.

26. Rigottier-Gois L, Madec C, Navickas A, Matos RC, Akary-Lepage E, Mistou MY, Serror P. 2015. The surface rhamnopolysaccharide epa of *Enterococcus faecalis* is a key determinant of intestinal colonization. J Infect Dis 211:62-71.

27. Li W, Xin Y, McNeil MR, Ma Y. 2006. *RmlB* and *rmlC* genes are essential for growth of mycobacteria. Biochem Biophys Res Commun 342:170-8.

28. Ma Y, Pan F, McNeil M. 2002. Formation of dTDP-rhamnose is essential for growth of mycobacteria. J Bacteriol 184:3392-5.

29. Engels W, Endert J, Kamps MA, van Boven CP. 1985. Role of lipopolysaccharide in opsonization and phagocytosis of *Pseudomonas aeruginosa*. Infect Immun 49:182-9.

30. Joiner KA. 1988. Complement evasion by bacteria and parasites. Annu Rev Microbiol 42:201-30.

31. Adibekian A, Stallforth P, Hecht M-L, Werz DB, Gagneux P, Seeberger PH. 2011. Comparative bioinformatics analysis of the mammalian and bacterial glycomes. Chem Sci 2:337-344.

32. Dong C, Beis K, Giraud MF, Blankenfeldt W, Allard S, Major LL, Kerr ID, Whitfield C, Naismith JH. 2003. A structural perspective on the enzymes that convert dTDP-d-glucose into dTDP-l-rhamnose. Biochem Soc Trans 31:532-6.

33. Dong C, Major LL, Allen A, Blankenfeldt W, Maskell D, Naismith JH. 2003. High-resolution structures of RmlC from *Streptococcus suis* in complex with substrate analogs locate the active site of this class of enzyme. Structure 11:715-23.

34. Giraud MF, Leonard GA, Field RA, Berlind C, Naismith JH. 2000. RmlC, the third enzyme of dTDP-L-rhamnose pathway, is a new class of epimerase. Nat Struct Biol 7:398-402.

35. Beis K, Allard ST, Hegeman AD, Murshudov G, Philp D, Naismith JH. 2003. The structure of NADH in the enzyme dTDP-d-glucose dehydratase (RmlB). J Am Chem Soc 125:11872-8.

36. Kantardjieff KA, Kim CY, Naranjo C, Waldo GS, Lekin T, Segelke BW, Zemla A, Park MS, Terwilliger TC, Rupp B. 2004. *Mycobacterium tuberculosis* RmlC epimerase (Rv3465): a promising drug-target structure in the rhamnose pathway. Acta Crystallogr D Biol Crystallogr 60:895-902.

37. Allard ST, Giraud MF, Whitfield C, Graninger M, Messner P, Naismith JH. 2001. The crystal structure of dTDP-D-Glucose 4,6-dehydratase (RmlB) from *Salmonella enterica* serovar Typhimurium, the second enzyme in the dTDP-l-rhamnose pathway. J Mol Biol 307:283-95.

38. Allard ST, Beis K, Giraud MF, Hegeman AD, Gross JW, Wilmouth RC, Whitfield C, Graninger M, Messner P, Allen AG, Maskell DJ, Naismith JH. 2002. Toward a structural understanding of the dehydratase mechanism. Structure 10:81-92.

39. Dong C, Major LL, Srikannathasan V, Errey JC, Giraud MF, Lam JS, Graninger M, Messner P, McNeil MR, Field RA, Whitfield C, Naismith JH. 2007. RmlC, a C3' and C5' carbohydrate epimerase, appears to operate via an intermediate with an unusual twist boat conformation. J Mol Biol 365:146-59.

40. Blankenfeldt W, Asuncion M, Lam JS, Naismith JH. 2000. The structural basis of the catalytic mechanism and regulation of glucose-1-phosphate thymidylyltransferase (RmlA). EMBO J 19:6652-63.

41. Babaoglu K, Page MA, Jones VC, McNeil MR, Dong C, Naismith JH, Lee RE. 2003. Novel inhibitors of an emerging target in *Mycobacterium tuberculosis*; substituted thiazolidinones as inhibitors of dTDP-rhamnose synthesis. Bioorg Med Chem Lett 13:3227-30.

42. Ma Y, Stern RJ, Scherman MS, Vissa VD, Yan W, Jones VC, Zhang F, Franzblau SG, Lewis WH, McNeil MR. 2001. Drug targeting *Mycobacterium tuberculosis* cell wall synthesis: genetics of dTDP-rhamnose synthetic enzymes and development of a microtiter plate-based screen for inhibitors of conversion of dTDP-glucose to dTDP-rhamnose. Antimicrob Agents Chemother 45:1407-16.

43. Ren JX, Qian HL, Huang YX, Zhu NY, Si SY, Xie Y. 2015. Virtual screening for the identification of novel inhibitors of *Mycobacterium tuberculosis* cell wall synthesis: inhibitors targeting RmlB and RmlC. Comput Biol Med 58:110-7.

44. Sivendran S, Jones V, Sun D, Wang Y, Grzegorzewicz AE, Scherman MS, Napper AD, McCammon JA, Lee RE, Diamond SL, McNeil M. 2010. Identification of triazinoindol-benzimidazolones as nanomolar inhibitors of the *Mycobacterium tuberculosis* enzyme TDP-6-deoxy-d-xylo-4-hexopyranosid-4-ulose 3,5-epimerase (RmlC). Bioorg Med Chem 18:896-908.

45. Wang Y, Hess TN, Jones V, Zhou JZ, McNeil MR, Andrew McCammon J. 2011. Novel inhibitors of *Mycobacterium tuberculosis* dTDP-6-deoxy-L-lyxo-4-hexulose reductase (RmlD) identified by virtual screening. Bioorg Med Chem Lett 21:7064-7.

46. Blankenfeldt W, Kerr ID, Giraud MF, McMiken HJ, Leonard G, Whitfield C, Messner P, Graninger M, Naismith JH. 2002. Variation on a theme of SDR. dTDP-6-deoxy-L- lyxo-4-hexulose reductase (RmlD) shows a new Mg2+-dependent dimerization mode. Structure 10:773-86.

47. Tsukioka Y, Yamashita Y, Oho T, Nakano Y, Koga T. 1997. Biological function of the dTDP-rhamnose synthesis pathway in *Streptococcus mutans*. J Bacteriol 179:1126-34.

48. Christendat D, Saridakis V, Dharamsi A, Bochkarev A, Pai EF, Arrowsmith CH, Edwards AM. 2000. Crystal structure of dTDP-4-keto-6-deoxy-D-hexulose 3,5-epimerase from *Methanobacterium thermoautotrophicum* complexed with dTDP. J Biol Chem 275:24608-12.

49. Stevenson G, Neal B, Liu D, Hobbs M, Packer NH, Batley M, Redmond JW, Lindquist L, Reeves P. 1994. Structure of the O antigen of *Escherichia coli* K-12 and the sequence of its rfb gene cluster. J Bacteriol 176:4144-56.

50. Graninger M, Nidetzky B, Heinrichs DE, Whitfield C, Messner P. 1999. Characterization of dTDP-4-dehydrorhamnose 3,5-epimerase and dTDP-4-dehydrorhamnose reductase, required for dTDP-L-rhamnose biosynthesis in *Salmonella enterica* serovar Typhimurium LT2. J Biol Chem 274:25069-77.

51. Ehmke N, Caliebe A, Koenig R, Kant SG, Stark Z, Cormier-Daire V, Wieczorek D, Gillessen-Kaesbach G, Hoff K, Kawalia A, Thiele H, Altmuller J, Fischer-Zirnsak B, Knaus A, Zhu N, Heinrich V, Huber C, Harabula I, Spielmann M, Horn D, Kornak U, Hecht J, Krawitz PM, Nurnberg P, Siebert R, Manzke H, Mundlos S. 2014. Homozygous and compound-heterozygous mutations in TGDS cause Catel-Manzke syndrome. Am J Hum Genet 95:763-70.

52. Tonetti M, Sturla L, Bisso A, Zanardi D, Benatti U, De Flora A. 1998. The metabolism of 6-deoxyhexoses in bacterial and animal cells. Biochimie 80:923-31.

53. Pferdehirt R, Jain M, Blazo MA, Lee B, Burrage LC. 2015. Catel-Manzke Syndrome: Further Delineation of the Phenotype Associated with Pathogenic Variants in TGDS. Mol Genet Metab Rep 4:89-91.

54. Schoner K, Bald R, Horn D, Rehder H, Kornak U, Ehmke N. 2017. Mutations in TGDS associated with additional malformations of the middle fingers and halluces: Atypical Catel-Manzke syndrome in a fetus. Am J Med Genet A 173:1694-1697.

55. Koga T, Asakawa H, Okahashi N, Takahashi I. 1989. Effect of subculturing on expression of a cell-surface protein antigen by *Streptococcus mutans*. J Gen Microbiol 135:3199-207.

Figure legends

Fig. 1 Schematic overview of streptococcal rhamnose polysaccharide structures.

Schematic representation of the chemical composition of the group A carbohydrate from GAS and the serotype c, e, f and k carbohydrates from *S. mutans* (SMU). All carbohydrates share an α-1,2/α-1,3 linked polyrhamnose backbone. Sugar residues in dashed boxes were recently identified by St Michael *et al*. (6).

Fig. 2 Protein sequence alignment and identity matrix of RmlB and RmlC homologs.

Color-coded representation of amino acid conservation for (A) GAS RmlB and (B) GAS RmlC to S. *enterica* and other streptococcal species. The amino acid conservation is scored from 0 to 10, with 0 (color blue) assigned to the least conserved residue and 10 (color red) to the most conserved residue. Critical enzymatic residues for RmlB (Y159) and RmlC (H76 and K82) are indicated with an inverted triangle. *S. pyogenes* (Spyo); *Salmonella enterica*; (Sent); *S. agalactiae* (Saga); *Streptococcus anginosus* (Sang); *Streptococcus dysgalactiae* (Sdys); *Streptococcus equi* (Sequ); *Streptococcus equinus* (Seqn); *S. mutans* (Smut); *S. pneumoniae* (Spneu); *Streptococcus suis* (Ssui). Protein accession numbers are described in the supplementary data (Table S2). (C) Percentage identity matrix of RmlB and RmlC homologs.

Fig 3. Heterologous expression of GAS RmlB and RmlC and catalytically-inactive enzymes in *S. mutans*.

(A, B) Growth curves, (C) representative scanning electron microscopy images and (D) cell wall carbohydrate composition analysis of *S. mutans* wild-type (SMU WT), SMU Δ*rmlB*, SMU Δ*rmlC*, SMU Δ*rmlB* + pSB, SMU Δ*rmlB* + pGB(_Y159F), SMU Δ*rmlC* + pSC and SMU Δ*rmlC* + pGC(_H76N/K82A). Rha, rhamnose; GlcNAc, N-acetylglucosamine; Glu, glucose. Growth curves represent mean ± standard error of mean (SEM) of at least three biological repeats.

Fig 4. Identified compounds inhibit growth of GAS.

(A) Dose-response curves for growth inhibition of GAS with various concentrations of Ri01, Ri02, Ri03, Ri06 or Ri08 to determine MIC_{50}. Values range between 110 µM to 2.66 mM. Dose-response curves represent mean ± SEM of at least three biological experiments performed in duplicate. (B) Representative scanning electron microscopy images of GAS after 16 h incubation in growth medium (THY), or THY with the addition of 1% DMSO, 0.2 mM Ri03 or 0.1 mM Ri06.

Fig. 5 Off-target effects of rhamnose inhibitors.

(A) Dose-response curves for growth inhibition of rhamnose-deficient *S. aureus* with various concentrations of Ri01, Ri02, Ri03, Ri06 or Ri08 to determine the MIC_{50}. Values range from 140 µM to 8.92 mM. (B) Release of lactose dehydrogenase by U937 monocytic cells after Ri03 exposure as a measurement for cytotoxicity. Dose-response and cytotoxicity curves represent mean ± SEM of at least three biological experiments performed in duplicate.

Table 1. Overview of identified compounds and MIC_{50} for GAS and *S. aureus*

Inhibitor	Compound	Binding target	MIC_{50} (mM) GAS	MIC_{50} (mM) *S. aureus*
Ri01	N-(1-Naphthyl)ethylenediamine dihydrochloride	RmlB + RmlC	0.27	0.68
Ri02	2,5-Difluorophenylhydrazine	RmlB + GacA	0.27	0.14
Ri03	5-(4-chlorophenyl)-2-furoic Acid	RmlB + GacA	0.12	2.48
Ri06	4,4'-Thiodiphenol	RmlB + GacA	0.11	0.44
Ri08	2-(2,5-Dimethyl-1H-pyrrol-1-yl)benzoic acid	RmlB +RmlC	2.67	8.92

Table 2. Bacterial growth inhibition by Ri03 in different bacterial species

Strain	MIC_{50} (mM)	Rhamnose
GAS 5448	0.12	Essential
S. mutans Xc	0.41	Critical
GCS MGCS10565	0.42	Essential
S. aureus NRS384	2.48	Absent
E. coli BW25113 WT	3.61	Non-essential
E. coli BW25113 Δ*rfb*A	3.74	Non-essential

Table 3. Bacterial strains used in this study

Bacterial strains	Abbreviation	Resistance
S. mutans Xc wild type (serotype c)	SMU WT	-
S. mutans Xc Δ*rmlB*	SMU Δ*rmlB*	ERY
S. mutans Xc Δ*rmlB* + pDC123_SMU_*rmlB*	SMU Δ*rmlB* + pSB	ERY + CHL
S. mutans Xc Δ*rmlB* + pDC123_GAS_*rmlB*	SMU Δ*rmlB* + pGB	ERY + CHL
S. mutans Xc Δ*rmlB* + pDC123_GAS_*rmlB*_Y159F	SMU Δ*rmlB* + pGB_Y159F	ERY + CHL
S. mutans Xc Δ*rmlB* + pDC123_*TGDS*	SMU Δ*rmlB* + pTGDS	ERY + CHL
S. mutans Xc Δ*rmlC*	SMU Δ*rmlC*	ERY
S. mutans Xc Δ*rmlC* + pDC123_SMU_*rmlC*	SMU Δ*rmlC* + pSC	ERY + CHL
S. mutans Xc Δ*rmlC* + pDC123_GAS_*rmlC*	SMU Δ*rmlC* + pGC	ERY + CHL
S. mutans Xc Δ*rmlC* + pDC123_GAS_*rmlC*_H76N	SMU Δ*rmlC* + pGC_H76N	ERY + CHL
S. mutans Xc Δ*rmlC* + pDC123_GAS_*rmlC*_K82A	SMU Δ*rmlC* + pGC_K82A	ERY + CHL
S. pyogenes 5448 wild type (serotype M1T1)	GAS	-
E. coli MC1061	-	-
E. coli BL21 (DE3)	-	-
E. coli DH5alpha	-	-
E. coli K-12 BW25113	Keio WT	-
E. coli JW2023 – Δ*rfbA* in BW25113	Δ*rfbA*	KAN
S. aureus USA300 NRS384	-	-
S. equi subsp. *zooepidemicus* MGCS10565	GCS	-

Figure 1

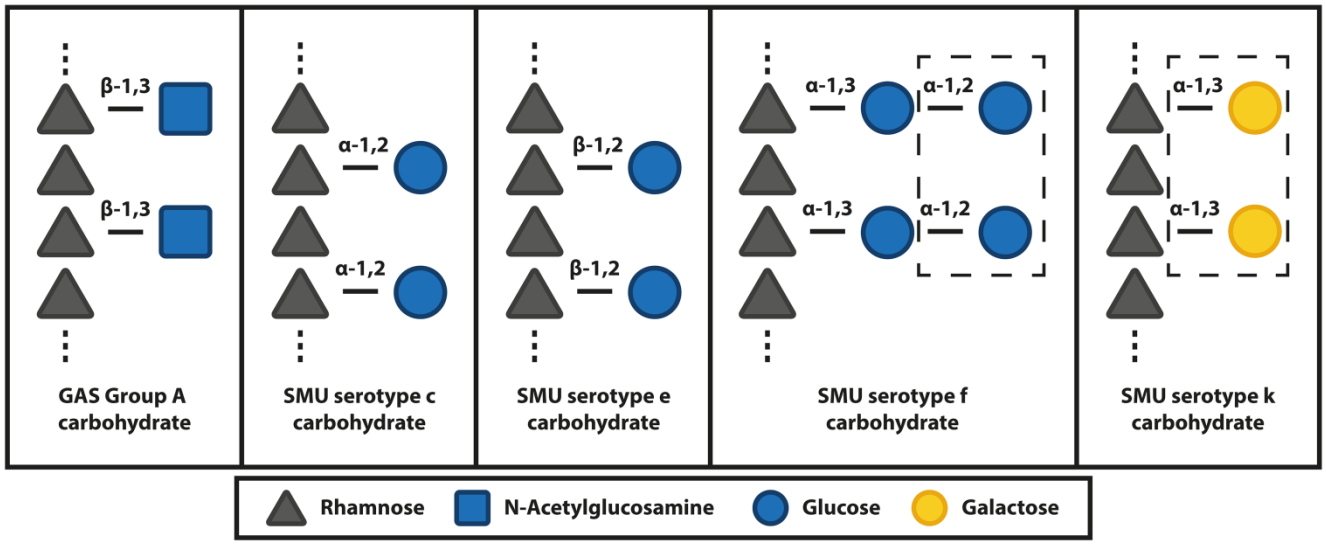

Fig. 1 Schematic overview of streptococcal rhamnose polysaccharide structures.
Schematic representation of the chemical composition of the group A carbohydrate from GAS and the serotype c, e, f and k carbohydrates from *S. mutans* (SMU). All carbohydrates share an α-1,2/α-1,3 linked polyrhamnose backbone. Sugar residues in dashed boxes were recently identified by St Michael *et al*. (6).

Figure 2

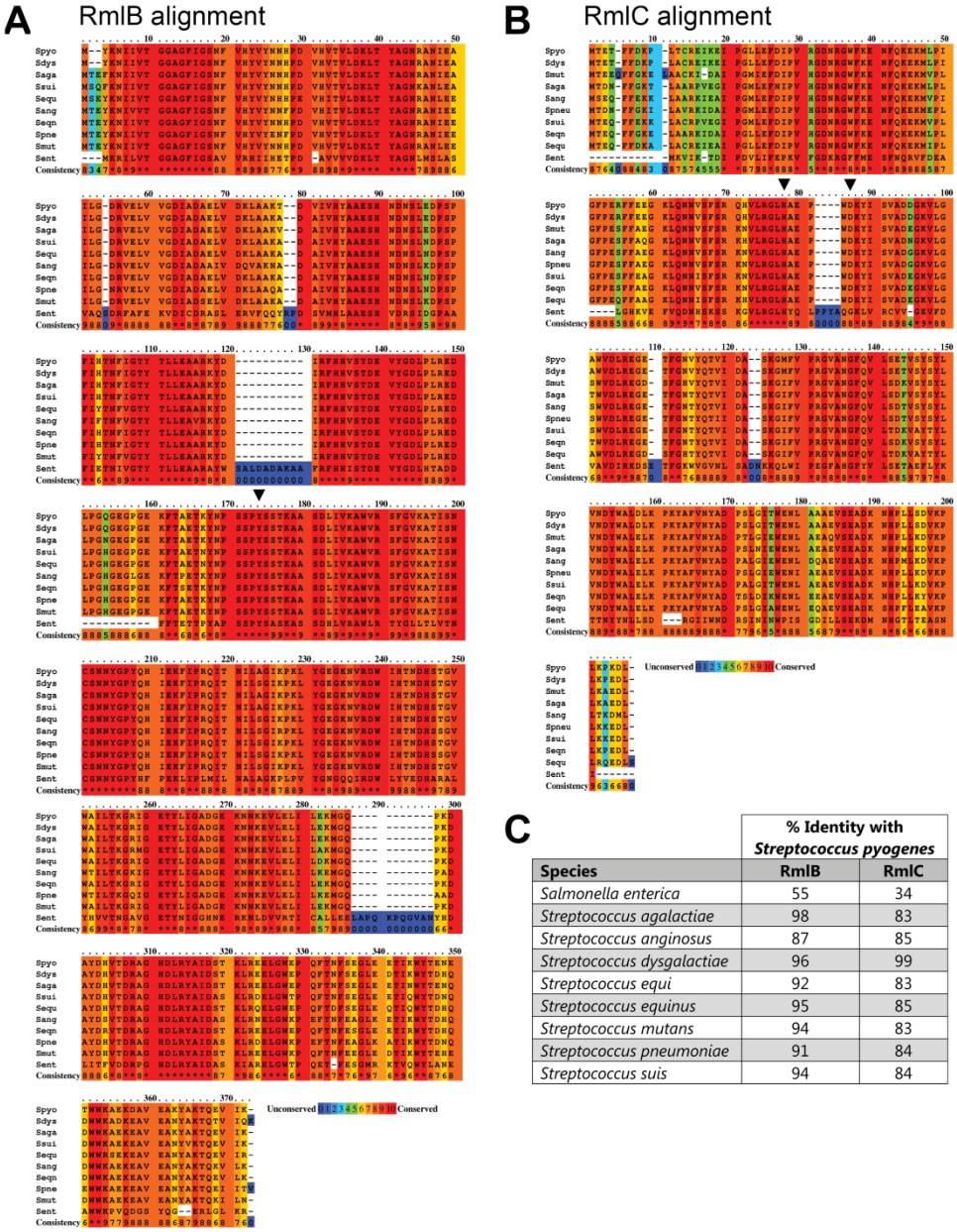

Species	% Identity with *Streptococcus pyogenes* RmlB	% Identity with *Streptococcus pyogenes* RmlC
Salmonella enterica	55	34
Streptococcus agalactiae	98	83
Streptococcus anginosus	87	85
Streptococcus dysgalactiae	96	99
Streptococcus equi	92	83
Streptococcus equinus	95	85
Streptococcus mutans	94	83
Streptococcus pneumoniae	91	84
Streptococcus suis	94	84

Fig. 2 Protein sequence alignment and identity matrix of RmlB and RmlC homologs.

Color-coded representation of amino acid conservation for (A) GAS RmlB and (B) GAS RmlC to *S. enterica* and other streptococcal species. The amino acid conservation is scored from 0 to 10, with 0 (color blue) assigned to the least conserved residue and 10 (color red) to the most conserved residue. Critical enzymatic residues for RmlB (Y159) and RmlC (H76 and K82) are indicated with an inverted triangle. *S. pyogenes* (Spyo); *S. enterica*; (Sent); *S. agalactiae* (Saga); *Streptococcus anginosus* (Sang); *Streptococcus dysgalactiae* (Sdys); *Streptococcus equi* (Sequ); *Streptococcus equinus* (Seqn); *S. mutans* (Smut); *S. pneumoniae* (Spneu); *Streptococcus suis* (Ssui). Protein accession numbers are described in the supplementary data (Table S2). (C) Percentage identity matrix of RmlB and RmlC homologs.

Figure 3

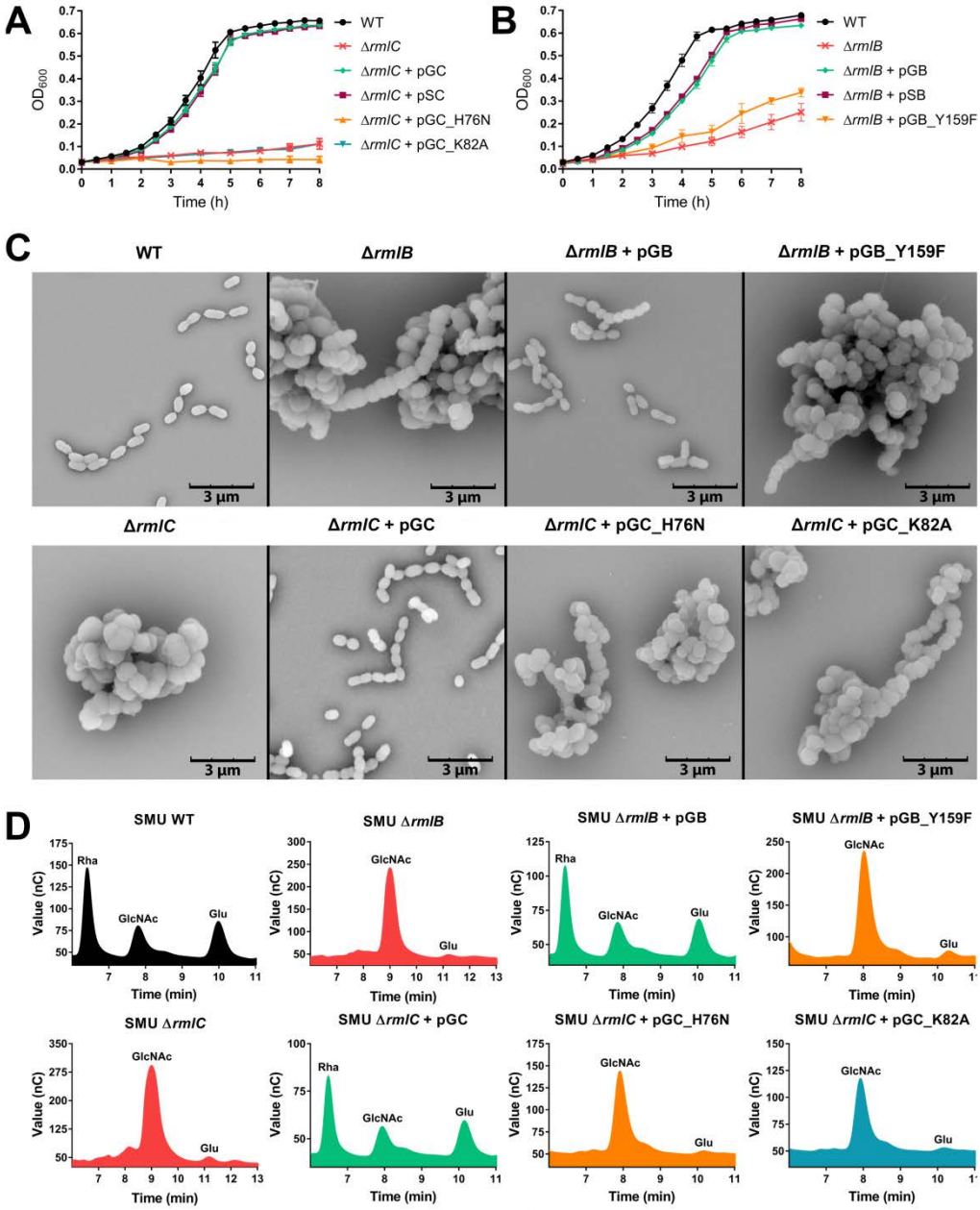

Fig 3. Heterologous expression of GAS RmlB and RmlC and catalytically-inactive enzymes in *S. mutans*.

(A, B) Growth curves, (C) representative scanning electron microscopy images and (D) cell wall carbohydrate composition analysis of *S. mutans* wild-type (SMU WT), SMU Δ*rmlB*, SMU Δ*rmlC*, SMU Δ*rmlB* + pSB, SMU Δ*rmlB* + pGB(_Y159F), SMU Δ*rmlC* + pSC and SMU Δ*rmlC* + pGC(_H76N/K82A). Rha, rhamnose; GlcNAc, N-acetylglucosamine; Glu, glucose. Growth curves represent mean ± standard error of mean (SEM) of at least three biological repeats.

Figure 4

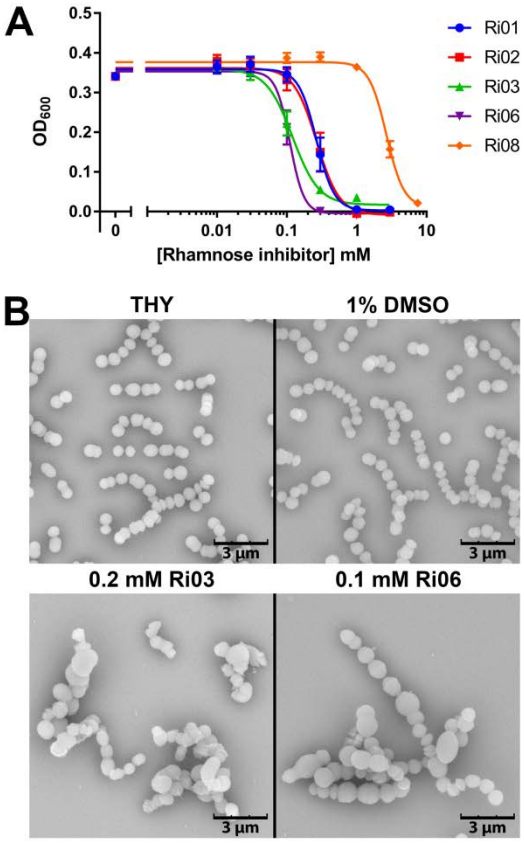

Fig 4. Identified compounds inhibit growth of GAS. (A) Dose-response curves for growth inhibition of GAS with various concentrations of Ri01, Ri02, Ri03, Ri06 or Ri08 to determine MIC_{50}. Values range between 110 µM to 2.66 mM. Dose-response curves represent mean ± SEM of at least three biological experiments performed in duplicate. (B) Representative scanning electron microscopy images of GAS after 16 h incubation in growth medium (THY), or THY with the addition of 1% DMSO, 0.2 mM Ri03 or 0.1 mM Ri06.

Figure 5

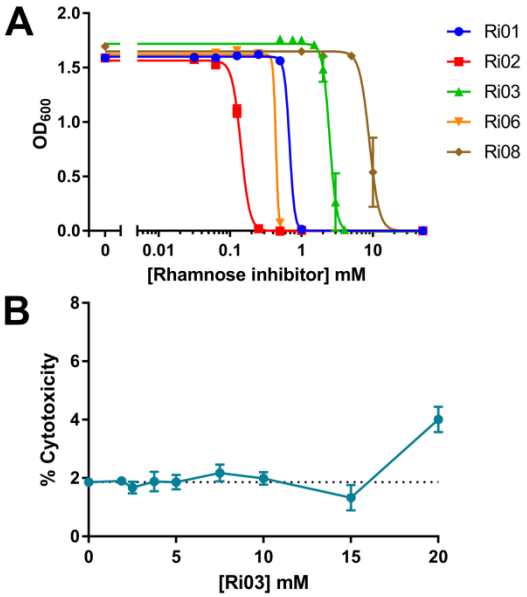

Fig. 5 Off-target effects of rhamnose inhibitors.
(A) Dose-response curves for growth inhibition of rhamnose-deficient *S. aureus* with various concentrations of Ri01, Ri02, Ri03, Ri06 or Ri08 to determine the MIC_{50}. Values range from 140 µM to 8.92 mM. (B) Release of lactose dehydrogenase by U937 monocytic cells after Ri03 exposure as a measurement for cytotoxicity. Dose-response and cytotoxicity curves represent mean ± SEM of at least three biological experiments performed in duplicate.